Available online at www.sciencedirect.com

SciVerse ScienceDirect

journal homepage: www.elsevier.com/locate/he

Modelling and simulation of wave energy hyperbaric converter (WEHC) for applications in distributed generation ☆

M. Martínez [*,a], M.G. Molina [b], I.R. Machado [c], P.E. Mercado [b], E.H. Watanabe [c]

[a] Instituto de Energía Eléctrica, Universidad Nacional de San Juan, Av. Libertador San Martín Oeste 1109, J5400ARL San Juan, Argentina
[b] CONICET, Instituto de Energía Eléctrica, Universidad Nacional de San Juan, Av. Libertador San Martín Oeste 1109, J5400ARL San Juan, Argentina
[c] COPPE, Power Electronics Group, Universidade Federal do Rio de Janeiro, Rio de Janeiro, Brazil

ARTICLE INFO

Article history:
Received 8 September 2011
Received in revised form
16 December 2011
Accepted 31 January 2012
Available online 2 March 2012

Keywords:
Sea wave energy
Wave energy hyperbaric converter (WEHC)
Dynamic modelling
Power conditioning system
Control scheme

ABSTRACT

The present work deals with the wave energy hyperbaric converter (WEHC) developed by the Federal University of Rio de Janeiro, Brazil. The development of WEHC, both for drawing energy from sea waves and for converting it into electrical energy, is based on keeping constant a pressure level within the hyperbaric accumulator (HA), which implies designing a large-size hyperbaric chamber (HC). Main objectives of this research are to reduce the size of the HC, and to obtain a high-quality level of the electrical output and a high flexibility degree for the WEHC. In this respect, power electronics, energy storage with super capacitors (SC) and their associated control play an important role to integrate the WEHC system to the electrical grid. The dynamics of the power conditioning system (PCS) influences on the validity of the WEHC system which acts, in turn, upon the dynamic control of the electrical power system, since it allows controlling the adequate power exchange between both systems. The proposed systems are analyzed and tested in simulations through SimPowerSystems from MATLAB/Simulink.

1. Introduction

Renewable energy sources are an alternative to respond to the electric power demand. Within these sources, power from sea waves gains importance as a solution for islands and countries having extensive coast areas [1].

This research employs the wave power converter developed at the Undersea Technology Laboratory of the Federal University of Rio de Janeiro, Brazil. It uses a hyperbaric accumulator (HA) together with hyperbaric chamber (HC) acting as power storage which, in turn, will smooth the power injected to the grid. A Pelton turbine (PT) driving an electric generator is used as the generating set. The optimal energy conversion with the Pelton turbine relies on keeping a constant pressure within the HA, which is achieved through a large-size HC [2]. This design significantly increases the overall costs, besides being very difficult to build. To overcome these constrains, this work proposes reducing the size of the hyperbaric chamber while compensating for the output power variations by incorporating a supercapacitor energy storage (SCES) device working altogether with a power conditioning system (PCS) in order to achieve a high-quality level of the electrical output from the WEHC system.

☆ This work was supported in part by MINCyT (Argentina) and CAPES (Brazil) under Scientific and Technological Cooperation Project BR/09/08.

* *Corresponding author*. Tel.: +54 264 4226444; fax: +54 264 4210299.
E-mail address: mmartinez@iee.unsj.edu.ar (M. Martínez).

0360-3199/$ – see front matter Copyright © 2012, Hydrogen Energy Publications, LLC. Published by Elsevier Ltd. All rights reserved.
doi:10.1016/j.ijhydene.2012.01.172

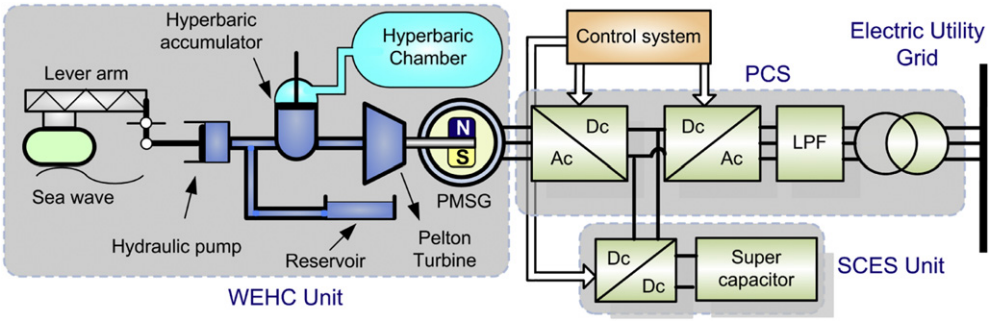

Fig. 1 – General components and layout of a WEHC system.

Based on these comments, the paper presents the development of a WEHC system for applications in distributed generation (DG) systems, which incorporates a novel power electronics interface and supercapacitor energy storage (SCES) device, altogether with an advanced control system designed for optimal energy capturing efficiency. The paper covers the detailed modelling of the WEHC, the power interface with the electric power grid and the design of the control system for the entire system. It also explains the analysis and its results of the dynamic performance of the WEHC.

2. Overview of the WEHC system

The WEHC system components and layout is depicted schematically in Fig. 1. It shows the WEHC unit, the SCES unit and the PCS for connecting to the electric grid. The WEHC, in turn, is composed of a pumping unit, the hyperbaric accumulator, the hyperbaric chamber, and a Pelton turbine coupled to a permanent magnet synchronic generator (PMSG). The SCES unit includes the super capacitor bank and a buck-boost converter. The PCS includes an AC/DC/AC back-to-back power converter built with voltage source inverters (VSIs).

The operating principle is based on using the buoy motion caused by the sea waves, transferring it through a cantilever beam arm to a set of pivoted levers linked to the piston of a hydraulic water pump. This pump absorbs treated water that is stored in a reservoir tank and its reverse stroke delivers this volume to the hyperbaric accumulator that is linked to the hyperbaric chamber. This water volume is then released at high pressure to the Pelton turbine -PMSG set for energy conversion. The articulated beam arm pumps the water only during the descending stroke, and this motion, induced by the action of gravity, overcomes the resisting force of the piston exerting the pressure needed to inject water to the hyperbaric accumulator under high pressure. This alternating motion renders the energy pulses in terms of hydraulic pressure stored in the high-pressure chamber. On the other hand, the storage capacity of the hydropneumatic system is crucial to support a flow with variations that can be governed by the PCS and the generation system. The PCS controls the rotation speed of the Pelton turbine in order to keep its maximum efficiency under fluctuations in water speed injected to the turbine, as a result of HA pressure variations. The power variations that the HC cannot smooth will be smoothed by the SCES storage unit.

3. Modelling the WEHC unit

3.1. *Pumping unit*

Modelling the pumping unit implies assuming a sinusoidal motion for the sea waves, and that the buoy speed $v_F(t)$ is in phase with the force exerted by the waves. In addition, the following constraints apply [2]:

- During pumping, the pressure on the piston is equal to the internal pressure of the HA.
- During the water intake by the pump, the pressure on the piston is equal to the atmospheric pressure.

The above premises allows assuming that the pump delivers a flow rate $Q_i(t)$ that follows a half sine wave. Eq. (1) models $Q_i(t)$, where the ascending motion is taken as positive and T is the period of the wave.

$$Q_i(t) = \begin{cases} 0, & v_F(t) > 0 \\ Q_i max \cdot sin\left(\frac{2\pi}{T}\cdot t\right) & v_F(t) < 0 \end{cases} \quad (1)$$

3.2. *Hyperbaric accumulator and hyperbaric chamber*

The hyperbaric accumulator contains water and air volumes separated by a piston, as shown in Fig. 2. When the input flow Q_i is greater than the output flow Q_o, the piston goes up and compresses the air volume. Conversely, when Q_o is greater than Q_i, the pistons goes down, thus decompressing the air mass.

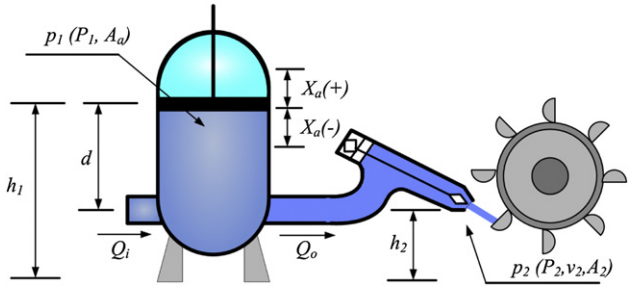

Fig. 2 – Hyperbaric accumulator (HA).

Therefore, the position of the internal piston of the accumulator $x_a(t)$ can be determined by the mass conservation law, as in Eq. (2), where A_a is the accumulator area [3]:

$$A_a\frac{dx_a(t)}{dt} = Q_i(t) - Q_o(t) \tag{2}$$

By neglecting the losses between the point p_1 of the HA (see Fig. 2) and point p_2 at the injector output, and applying Bernoulli's Equation, the following equality can be found:

$$P_1 + \frac{1}{2}\rho v_1^2 + \rho g h_1 = P_2 + \frac{1}{2}\rho v_2^2 + \rho g h_2 \tag{3}$$

Where P, ρ, v, g and h represent the pressures, density, speeds, gravity acceleration and liquid heights, respectively.

Considering $v_1 = 0$, and P_2 equal to the atmospheric presure, Eq. (4) is obtained, where d is the initial height of the water inside the HA.

$$v_2(t) = \sqrt{2\left[g(d + x_a(t)) + \left(\frac{P_1(t) - P_2}{\rho}\right)\right]} \tag{4}$$

In order to model the HC, the following assumptions are made: the air is a perfect gas, the transformations are isothermal and the air mass is constant. With these suppositions and considering the perfect gas state equation, it is possible that the variation of $P_1(t)$ be represented by Eq. (5). There, P_0 is the initial pressure of the air and V_T is the total volume of the HA + HC set. Finally, the output flow rate $Q_o(t)$ is shown in Eq. (6), with A_2 being the output area of the injector nozzle [3].

$$P_1(t) = P_0\left(\frac{V_T - d\cdot A_a}{V_T - (d + x_a(t))\cdot A_a}\right) \tag{5}$$

$$Q_0(t) = v_2(t)\cdot A_2 \tag{6}$$

3.3. Pelton turbine

By neglecting the friction losses in the spoons of the turbine wheel, and using the values of speed v_2 and flow rate Q_o, it is possible to express the mechanical torque T_m produced by the wheel, trough Eq. (7).

$$Tm = R(v_2 - \omega_r R)(1 - \cos\beta)\rho Q_O \tag{7}$$

There, R is the turbine radious, ω_r is the angular speed of the turbine and β is the angle formed by the tangential speed u of the turbine and the relative speed w of water diverted by the spoons.

By multiplying Eq. (7) by ω_r, the value of mechanical power can be found. It is null for $\omega_r = 0$ and for $\omega_r = v_2/R$. Therefore, the maximum power transfer will lay between these two values. Hence, by applying derivatives to Eq. (8) as a funtion of ω_r and equating this expression to zero, the value of ω_r for maximum power transfer is obtained using Eq. (9) [4].

$$Pm = \omega\cdot R(v_2 - \omega_r R)(1 - \cos\beta)\rho Q_O \tag{8}$$

$$\omega_r = \frac{v_2}{2\cdot R} \tag{9}$$

3.4. Permanent magnet synchronic generator (PMSG)

Eq. (10) through (12) model electrically the dynamic performance of the PMSG in $dq0$ coordinates. There, L_q and L_d represent the inductances, i_d and i_q the currents, u_q y u_d the voltaje values on axes d and q, respectively. The number of pole pairs is p_P, R_S is the stator resistance, ψ is the amplitude of the flux induced by the permanent magnet rotor on the stator coils, ω_r is the angular speed of the rotor, and M_{em} is the electromagnetic torque. Eq. (13) represents the mechanical model, where J is the electric motor's inertia and C_{fm} is its friction coefficient [5].

$$v_d = R_S i_d + L_d\frac{di_d}{dt} - \omega_r L_q i_q \tag{10}$$

$$v_q = L_q\frac{di_q}{dt} + R_S i_q + L_d\omega_r i_d + \psi\omega_r \tag{11}$$

$$M_{em} = 1,\ 5\cdot p_P\left[\psi\cdot i_q + (L_d - L_q)\cdot i_d\cdot i_q\right] \tag{12}$$

$$\frac{d}{dt}\omega_r = \frac{1}{J}(M_{em} - C_{fm}\omega_r - M_m), \tag{13}$$

4. SCES unit

The integration of the SCES unit requires of a DC/DC buck-boost converter, as shown in Fig. 3. The DC/DC converter (chopper) features two operating modes: the charging mode (buck) and the discharging mode (boost). In buck mode, the IGBT T_{bck} is switched on, while keeping IGBT T_{bst} switched off all the time, so as to allow a charging current flow to the SC bank. In boost mode, T_{bst} is switched on while keeping T_{bst} switched off so as to let the discharge of the SC bank. Eq. (14) relates the mean output voltage V_{SCB} to the the DC bar voltage (V_d), having a modulation index $m = D$ for the buck mode and $m = (1–D)$ for the boost mode. D is the operating relationship to switch on/off T_{bck} or T_{bst} according to the operating mode (charge or discharge) [6].

$$V_{SCB} = m\cdot V_d \tag{14}$$

5. Power conditioning system (PCS)

The power conditioning system (PCS) shown in Fig. 3, is composed of a back-to-back AC/DC/AC converter. Two three-phase three-level voltage source inverters (VSI) based on IGBTs are proposed to produce the AC/DC/AC conversion [7]. The connection to the power grid is made through a transformer and a low-pass filter so as to reduce the harmonics resulting from the high-frequency switching.

Both three-level VSIs are controlled by PWM sinusoidal switching techniques. The VSI linked in parallel to the power grid uses for such connection an inductance L_s, that represents the equivalent dispersion flux of the transformer, plus a series resistance R_S representing the resistance of transformer coils and the losses at the VSI semiconductor devices. The magnetization inductance of the transformer is also taken into account by the mutual inductance M. The

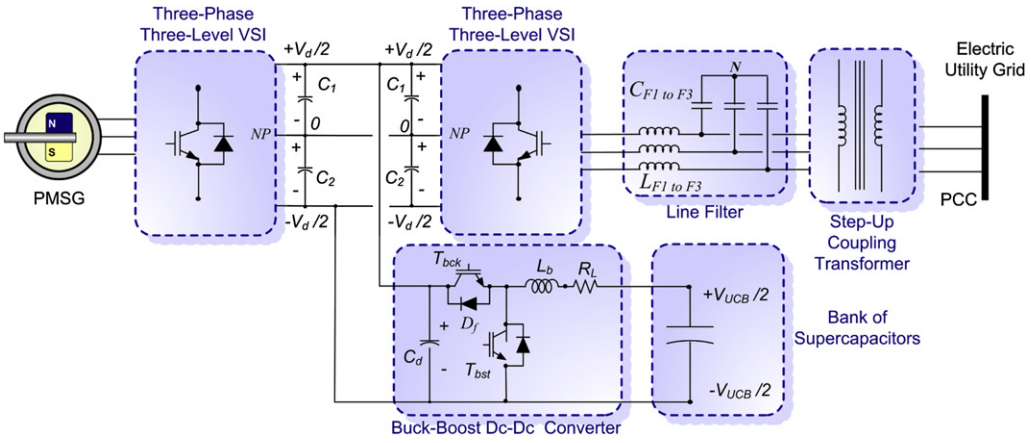

Fig. 3 – Detailed model of the SCES unit and the PCS.

dynamics of the system can be summed up in the state space Eq. (15).

$$s\begin{bmatrix} i_d \\ i_q \\ V_d \end{bmatrix} = \begin{bmatrix} \frac{-R_s}{L_s - M} & \omega & \frac{mi.a\cos\alpha}{2(L_s - M)} \\ -\omega & \frac{-R_s}{L_s - M} & \frac{mi.a\sin\alpha}{2(L_s - M)} \\ -\frac{3mi.a\cos\alpha}{2C_d} & -\frac{3mi\cdot a\sin\alpha}{2C_d} & \frac{2}{R_p C_d} \end{bmatrix} \times \begin{bmatrix} i_d \\ i_q \\ V_d \end{bmatrix} - \begin{bmatrix} \frac{|v|}{L_s - M} \\ 0 \\ 0 \end{bmatrix} \quad (15)$$

In this equation, V_d is the DC link voltaje, ω is the synchronous angular speed of the grid voltage, m_i is the modulation index ($m_i \in [0, 1]$), a is the voltage ratio of the coupling transformer, and α is the phase shift of the VSI output voltage respecting the reference position [5].

6. Control strategy

The proposed multi-level control scheme for the three phase grid-connected WEHC system is depicted in Fig. 4 This three-level control consists of external, middle and internal level, with different hierarchies between them. The control is based on concepts of instantaneous power on the synchronous-rotating dq reference frame.

6.1. External level control

The external level control governs the active and reactive power exchange between the WEHC system and the electric grid, using an active power control mode (APCM) and a voltage control mode (VCM) [5]. The purpose of the APCM is to control de operating point of the pelton turbine. The dynamic behavior of the electromechanical system is shown in Eq. (16), where C_f is the total friction coefficient, J_T is the total inertia and $\dot{\omega}_r$ is the angular acceleration.

$$J_T\dot{\omega}_r = M_m - C_f\omega_r - M_{em} \quad (16)$$

On the basis of having determined the position of the HA piston, the calculation module of the optimal rotation speed (MCORS) allows finding the rotation speed of the PT wheel at which it delivers maximum power. This value is converted into a reference torque M_{emr} by means of a speed regulator that adjusts the real speed to the reference speed proposed by the MCORS. The VCM is designed to control the voltage in the common coupling point (PCC), through the modulation of the reactive component of the output current (fundamental quadrature component, i_{qr1}).

6.2. Middle level control

The middle level control makes the expected output to dynamically track the reference values set by the external level. As it can be noted from Eq. (15), there is a cross-coupling of both components of the VSI output current through ω. In order to achieve a full decoupled control of the active and reactive power, the signals X_1 y X_2 are used (AC side). In order to reach this condition in steady state, two PI controllers are introduced, having adequate feedback of i_{d1} e i_{q1}, as shown in Eq. (17) below:

$$s\begin{bmatrix} i_d \\ i_q \end{bmatrix} = \begin{bmatrix} \frac{-R_s}{L_s - M} & 0 \\ 0 & \frac{-R_s}{L_s - M} \end{bmatrix} \begin{bmatrix} i_d \\ i_q \end{bmatrix} - \begin{bmatrix} X_1 \\ X_2 \end{bmatrix} \quad (17)$$

From Eq. (15), it can be seen the additional coupling resulting from the DC voltage, both on the DC side and on the AC one. This requires keeping V_d constant so as to decrease the dynamic influence of V_d. The solution is to employ a PI compensator that eliminates the voltage variations on the DC bus [5]. On the other hand, the VSI AC/DC middle control is built with four main blocks. The torque-to-current converter block in $dq0$ coordinates converts M_{emr} into a current i_{qr} ($M_{em} = 1.5\ P\ \psi\ i_q$), on account for the type of machine employed. The current i_d is set equal to zero. The block dq-abc performs the conversion of the referente system $dq0$ into the abc coordinates. The current regulating block is a bang–bang current controller with adjustable hysteresis band width [6]. The angle converter block is used to compute the electrical angle of the rotor.

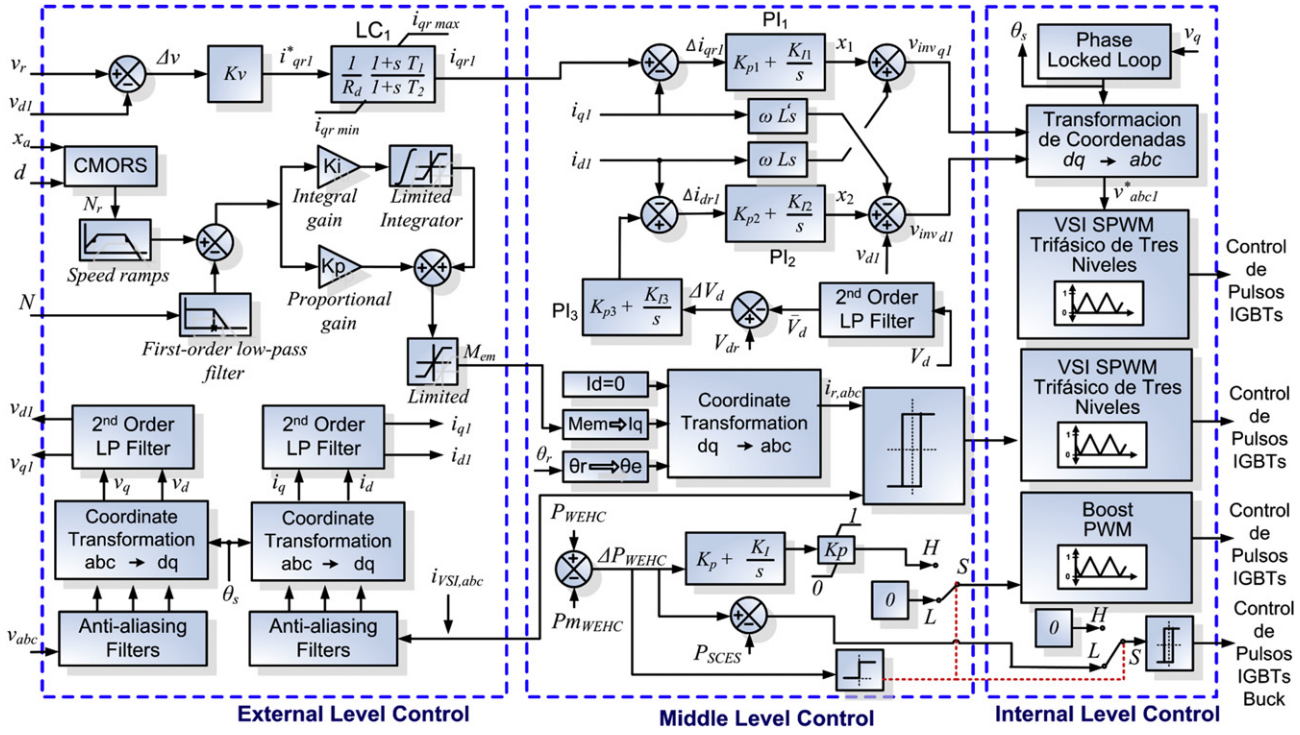

Fig. 4 – Multilevel control scheme of the WEHC system.

The buck or boost mode, as well as the charge or discharge power of the SCES unit is determined by the subtraction between the mean power and the instantaneous power developed by the WEHC unit (ΔP_{WEHC}). When this value is positive, the switch *S* goes to position *L* and when it is negative it goes to position *H*.

Since the supercapacitors current is very sensitive to the applied voltage, a technique of adaptive hysteresis current control (AHCC) is proposed to operate the DC/DC converter in continuous condution mode. This way, charging the SCES is fast at a constant power close to ΔP_{WEHC}. In the boost mode, the ΔP_{WEHC} becomes the reference discharge current via a PI controller that adjusts the power delivered by the supercapacitor to ΔP_{WEHC}, by means of regulating the duty cycle *D*.

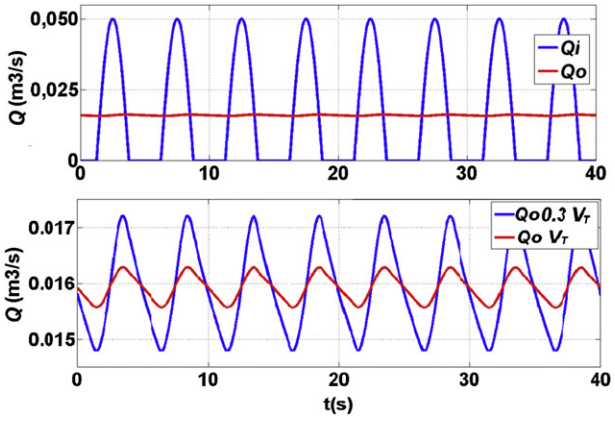

Fig. 5 – Hyperbaric accumulator input and output flow rates.

6.3. *Internal level control*

This level is responsible of generating the switching signals for the VSI valves and for the DC/DC converters, according to the sinusoidal PWM control modes and the AHCC, as well as the type of switch employed (IGBT). This level is built with a line synchronization module, two thre-phase three-level SPWM firing pulses generators, one PWM firing pulse generator and one hysteresis firing pulse generator. The line synchronization module consists mainly of a phase locked loop (PLL) [5].

7. Digital simulations

Simulations were performed using SimPowerSystems of MATLAB/Simulink [8], considering a sine wave having a period $T = 5s$, a $Q_{imax} = 0.0502\ m^3/s$, an initial interal pressure $P_1(0) = 58.8e^5\ N/m^2$, $P_2 = 1e^5\ N/m^2$, $Aa = 0.64\ m^2$, $A_2 = 1.48e^{-4} m^2$, $V_T = 1\ m^3$, $d = 0.5$ m, $R = 0.38$ m, $\rho = 1000$ kg/m^3, $g = 9.8$ m/s^2, and $\beta = 2.61$ rad.

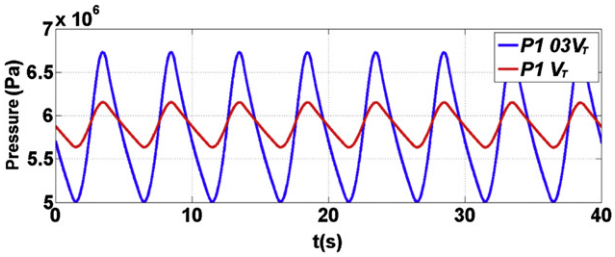

Fig. 6 – Hyperbaric accumulator internal pressure.

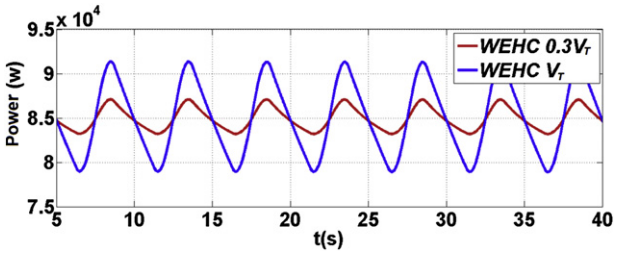

Fig. 7 – Power delivered to the electric grid by the WEHC.

Fig. 5 shows the input flow rate Q_i and output flow rate Q_o of the HA, with volumes V_T and $0.3V_T$, respectively. It can be noted a mean Q_o of 0.0159 m^3/s and an oscillation of 2.2% for $1.0V_T$ and 7.8% for $0.3V_T$. In the same way, Fig. 6 shows a mean pressure of $58.87e^5N/m^2$ within the AH, with a 4.5% swing for $1.0V_T$ and a mean pressure of $57.88e^5N/m^2$ and 16% swing for $0.3V_T$. Eventually, Fig. 7 depicts the variations in power delivered to the distribution network by the traditional WEHC for $1.0V_T$ and that of the proposed WEHC for $0.3V_T$. It can be seen that the proposed system generates the same mean power of 85 kW with an oscillation of 2.5% as opposed to 7.5% of the traditional WEHC.

8. Conclusions

This work presented the design of a sea wave energy hyperbaric converter combined with a supercapacitor energy storage bank in order to improve the quality of the electrical power delivered to the distribution network. The proposed design allowed reducing the total volume of the hyperbaric accumulator and hyperbaric chamber to about 30% of its value which, in turn, increases about 9% the peak pressure and output flow rate oscillations from 2.2 to 7.8%. The combination of the PCS and the SCES unit enabled to lessen the disadvantageous features of former designs, while obtaining an output power response that is smoother than that of the traditional WEHC. These improved characteristics of the proposed system confirm its better adequacy for distributed generation applications.

REFERENCES

[1] Falnes J. Principles for capture of energy from ocean waves. Phase control and optimum oscillation. Technical report. Department of physics, Norwegian University of Science and Technology. Available from:, www.ntnu.no; 1997.
[2] Garcia-Rosa PB, Cunha JPVS, Lizarralde F, Estefen SF, Costa PR. Efficiency optimization in a wave energy hyperbaric converter. Proc. Int. Conf. on Clean Electrical Power; 2009. pp. 68–75.
[3] Machado IR, Bozzi FA, Watanabe EH, Garcia-Rosa PB, Martínez M, Molina MG, et al. Wave energy conversion system using asynchronous generators – a comparative study. Proc. Brazilian Power Electronics Conference; 2011 (COBEP '11), pp. 286–291.
[4] Fernández Díez P. Turbina pelton (In Spanish). Technical report. España: Department of Electrical and Energy Engineering, University of Cantabria. Available from: http://es.libros.redsauce.net/; 2003.
[5] Molina MG, Mercado PE. Modelling and control design of pitch-controlled variable speed wind turbines. In: Al-Bahadly I, editor. Wind Turbines. Vienna: In Tech Ed. & Pub; 2011. p. 373–402.
[6] Molina MG, Mercado PE. Power flow control of microgrid with wind generation using a DSTATCOM-UCES. Proc. IEEE International Conference on Industrial Technology; 2010 (ICIT'10), pp. 955–960.
[7] Rodriguez J, Lai JS, Peng FZ. Multilevel inverters: a survey of topologies, controls, and applications. IEEE Trans On Industrial Electronics 2002;49(4):724–38.
[8] The MathWorks Inc. SimPowerSystems for use with Simulink: user's guide. Available from: www.mathworks.com; 2011.